PERGAMON

Radiation Measurements 30 (1999) 589–597

Radiation Measurements

www.elsevier.com/locate/radmeas

A multi-spacecraft synthesis of relativistic electrons in the inner magnetosphere using LANL, GOES, GPS, SAMPEX, HEO and POLAR

R.H.W. Friedel[a,*], G. Reeves[c], D. Belian[c], T. Cayton[c], C. Mouikis[a], A. Korth[a], B. Blake[b], J. Fennell[b], R. Selesnick[b], D. Baker[d], T. Onsager[e], S. Kanekal[f]

[a]*Max-Planck-Institut für Aeronomie, Katlenburg-Lindau, Germany*
[b]*The Aerospace Corporation, El Segundo, CA, USA*
[c]*Los Alamos National Laboratory, Los Alamos, NM, USA*
[d]*LASP, Boulder, CO, USA*
[e]*NOAA/SEC, Boulder, CO, USA*
[f]*NASA/GSFC, Greenbelt, MD, USA*

Received 30 August 1998; accepted 12 March 1999

Abstract

One of the Brussels Radiation Belt Workshop recommendation was the establishment of a near-real-time data driven model of the inner magnetospheric energetic particle population ($L < 8$). Although the "ideal" missions and data sets for such a model do not exist at present, more spacecraft than ever before are currently sampling the inner magnetosphere. We attempt here in a case study of the 10 January, 1997 magnetic cloud event to construct such a model with the energetic electron data available from 5 geosynchronous and 6 elliptically orbiting satellites. We examine the constraints and difficulties of putting together a large number of datasets which are measured near-simultaneously at very different locations in the inner magnetosphere. First results indicate that we can achieve a time resolution of about 3 h for a given "snapshot" of the inner magnetosphere, and that large azimuthal asymmetries of the energetic electron population can be observed during large storms.

1. Introduction

In the current era of the International Solar Terrestrial Program (ISTP) a large number of concurrent missions are flown (POLAR, EQUATOR-S, GEOTAIL, WIND, INTERBALL, SAMPEX) in addition to the already existing programs such as the GOES and Los Alamos National Laboratory geostationary platforms and the NOAA spacecraft. While the ISTP spacecraft are dedicated science missions and carry excellent instrumentation for the detection and characterization of the radiation environment in the inner magnetosphere, the others carry somewhat simpler environmental monitors for the detection of hard radiation.

Traditionally data from a given instrument are analyzed in isolation, and comparisons to data from other instruments on other spacecraft are performed on an

* Corresponding author. Present address: Los Alamos National Laboratory, Los Alamos, NM 87544, USA.

1350-4487/99/$ - see front matter
PII: S1350-4487(99)00230-9

event basis only. The main reason for such limited inter-comparisons has been the difficulty of the task. Instrument operators had a hard enough time understanding their own instruments — and for many studies absolute flux values were not needed.

With the wealth of data being returned by today's satellites from the inner magnetosphere there is an opportunity to put this data together on a more routine basis. This in effect requires all of the tasks that were needed for event studies — across many more instruments and satellites. This is a daunting task and one that cannot be accomplished without some simplifying assumptions. The aim of this work is to obtain a global representation of the radiation environment in the inner magnetosphere, based on actual data from as many input sources as possible, and yielding a complete picture with as high a time resolution as possible. This is a radical departure from the statistical models such as NASA's AE-8 (Vette, 1991) or CRRES-based models, or the physical models such as SALAMMBO {Beutier and Boscher, 1995}, the Rice Specification Model, or any other MHD code. The statistical approach by its nature yields an average picture, while the modeling approach yields an idealized picture.

This paper investigates a synthesis between actual data and some simple physical principles to yield a highly realistic picture of the environment as it actually was. Initially this will be done for past times, using already existing data as input, with the aim of moving as close to real time as the respective data streams from the satellites allow. We further need to move away from the traditional time-series representation of the data and explore new tools to meaningfully represent such a global view of the radiation environment governing the spatial, temporal and energy dimensions.

This procedure will eventually become an invaluable space weather tool, providing environmental "snapshots" of the state of the magnetosphere very much analogous to the traditional weather maps for terrestrial weather. These data can then be used as a basis of forecast or as accurate specification of the past environment, as is needed for the post-event analysis carried out to determine the source of spacecraft operating errors.

From a scientific point of view such data can provide important insights into the global development of magnetic storms, in particular the asymmetric filling of the radiation belts. A further important by-product is an ongoing inter-calibration of many data sets, which can aid in the debugging and quality control of the individual instruments.

2. Synthesis procedure

We outline here the "perfect" union of many data sets, and show in how many ways even simple requirements cannot be met, and how many approximations become necessary in order to proceed.

The underlying physical concept used here is that of drift shells. In the inner magnetosphere, when the global magnetic field is slowly varying, all three adiabatic invariants can be conserved for prolonged times. Here "slowly" means within a couple of hours — the time it takes to get sufficient coverage for a global map. Energetic particles are virtually unaffected by electric fields and their motion is governed only by the magnetic field. Particles will stay on a given drift shell and orbit the Earth for many orbits. In the steady state a drift shell will be equally filled at all magnetic local times (MLT), thus a single point measurement yields information about the whole drift shell. As a reference, this measurement point can always be mapped to the geomagnetic equator. This point then uniquely defines the fluxes *everywhere* on this drift shell. This principle was used by Friedel and Korth (1994, 1995, 1996); and Korth et al. (1998) to yield one-dimensional L-profiles of the radiation belts based on CRRES measurements.

During dynamic times, however, particles can be injected locally at one MLT and require some time to isotropize along the drift shell. Then one needs multi-MLT measurements and the condition of drift shell uniformity breaks down. On the time scale of one drift period (in the order of tens of minutes for relativistic electrons >2 MeV) particles do not diffuse radially, so an interpolation along the drift shell between measurements is a good representation of the instantaneous fluxes along a drift shell.

Once a good representation of *one* drift shell has been found, this can be used as an equatorial reference "ring", in order to tie in data from spacecraft with more radial coverage. In an utopian world of perfect calibrations the fluxes measured by a satellite radially traversing this "ring" should agree with the values of the reference ring (when mapped to the equator).

One can now add in as many radial crossings of this reference ring as possible within a given time period. Here there is a tradeoff. For a global map to work one has to assume that the system is stationary for the period chosen — thus the shorter the period, the better this assumption. However, if the time period chosen is too small not enough spacecraft actually intersect the reference ring, and their radial coverage is small. If the period is too large the assumption of stationarity breaks down.

Once these radial components have been added in one can proceed to fill in the data for drift shells other than the reference ring, again interpolating between points of measurement along drift shells, all mapped to the equatorial plane. This then finally yields a complete map of the state of the inner radiation belts for the time period chosen.

This method does have a catch though. Our defi-

nition of a drift shell is dependent on the magnetic field model used — which again is an approximation to the real dynamic field. In our approach here we start with a static model, accepting that this breaks down during very disturbed times. Adding in a time-dependent magnetic field model is left as the next step.

The application of this method to obtain such a map for relativistic electrons >2 MeV requires the steps summarized below:

1. Well calibrated flux spectra for each satellite are needed. Based on a fit through the discrete or integral channels an equivalent >2 MeV channel is constructed from each instrument. Ideally we need the full distribution function — as this is not available from many spacecraft omni-directional fluxes are used.
2. For all satellites an equivalent set of magnetospheric ordering parameters (L, MLT, MagLat) needs to be constructed based on the same magnetic field model.
3. All fluxes need to be transformed to equatorial fluxes using either a theoretical or statistical model.
4. A "base-ring" is constructed near geostationary orbit since here the coverage is most comprehensive (LANL, GOES, UARS).
   4.1. All measurements are scaled to agree at 12 MLT during quiet times. Quiet time is used since the spacecraft go through 12 MLT at different times, in order to have the same ambient conditions.
   4.2. Geostationary is almost equal to a drift shell at $L = 6.6$: Use closest radial profile (in space and time) to adjust fluxes.
   4.3. Fluxes are linearly interpolated from satellite to satellite forming a ring of fluxes at $L = 6.6$
5. All non-geosynchronous satellites are searched for geostationary crossings in the given time window.
6. Orbits are segmented into individual crossings through L for this time window (needed for low orbit satellites with more than one orbit during the time window)
7. Fluxes along each L-slice are "anchored" at the geostationary base-ring by transforming them to the equator and using the geostationary fluxes at that MLT as a reference. Only fluxes above a threshold are used to avoid scaling to each other's background.
8. Fluxes at all L are interpolated at a given L along MLT between the radial slices forming a complete snapshot at all L, MLT.
9. The process is repeated in some time increments.

The final series of "snapshots" can then be viewed as a movie. To increase time resolution, a linear interpolation between such frames in time can be employed.

2.1. Limitations and approximations - the real world

In order to have some result in a reasonable length of time we needed to severely compromise on the idealized procedure described above. As our initial aim is to show the usefulness of our approach we decided use a test period for which a lot of data was available — the January 1997 Storm (Reeves et al., 1998). This was an extremely active and disturbed period during which the stationary assumption was clearly violated at times, but the lengthy procedure of gathering together data was avoided.

The data used here come from a variety of instruments and missions. As our interest is in measuring "dangerous" radiation we chose here relativistic electrons of energies >2.0 MeV.

For none of the instruments calibrated spectra were available to yield the "same" energy channel for each instrument. As this is very much up to the instrument PI to provide we did not attempt to do this ourselves. We chose the data channel in each instrument which was closest to >2.0 MeV.

Furthermore, the data came from instruments with different angular coverage and response, in either flux or counts. The list below shows the instruments/channels used:

1. Los Alamos geostationary satellites ESP (Energetic Spectra for Particles). Omni-directional flux (Reeves et al., 1997). 1990–095, 1991–080, 1994–084, all >1.8 MeV electrons
2. GOES geostationary satellites. Omni-directional flux (Space-Systems-Loral, 1996). GOES-8, GOES-9, both >2.0 MeV electrons
3. SAMPEX >1.0 MeV electrons. 600 km 83° inclination polar orbit. Precipitating flux (Baker et al., 1993).
4. HEO >1.5 MeV electrons. Highly elliptical (1.1×7 R_e) 12 h orbit. Omni-directional flux. For a description see in Blake et al. (1997)
5. POLAR 1.9–10 MeV CEPPAD HISTe {Blake et al., 1995}. Polar (2×9 R_E) 18 h orbit. Omni-directional flux.
6. GPS electrons BDD [Burst Detector Dosimeter (Feldman et al., 1985)]. Twelve hour geostationary transfer orbit, incl. 45°. Half hemisphere counts. ns39, ns33, ns24, all 1.6–3.2 MeV

Given these restrictions on the data we adopted a simple scaling strategy. All the geostationary satellites had basically identical channels and well calibrated data. They agreed to within factors of 2 at 12 MLT during quiet times. We arbitrary chose one satellite with factor unity and scaled the fluxes of all the others accordingly.

All the other satellite data was then scaled to the geostationary "ring" using linear scaling factors. The

basic assumption here is that for isotropic distributions (and electron distributions are mainly isotropic) the measurements of omni directional flux have a linear relationship to the measurements of any other angular subset of the distribution in either counts OR flux.

Most of the data was accompanied by some "L" value. For some data it was not possible to find out how this had been calculated. A simple dipole "L" was used when L was not available.

For the geostationary data in a dipole field all MLT are at the same L by definition. This again is a first approximation.

Shown here in Fig. 1 are the original un-scaled input data for the data synthesis. In this format it is very difficult to get a "global" picture of the flux changes throughout the inner magnetosphere. The increase in flux is clearly seen at geostationary near 16:00 h on 11 January 1997, and shows up at all satellites. Each satellite is at a different MLT and "sees" this event differently - but it is impossible to get a global picture of this event from this plot alone.

2.2. Method used (real world)

An initial synthesis was attempted even though not all the conditions of the "idealized" method could be achieved:

1. Only for HEO, SAMPEX, LANL and GOES were the measurements available in fluxes. POLAR fluxes are based on preliminary geometric factors. GPS is in counts.
2. The exact energy range of >2 MeV was only approximated by the nearest integral or differential channel available. For none of the instruments a fully calibrated spectral fit was available.
3. Calculation of common magnetic field parameters for all satellites has not been performed yet. L values as delivered with the data where used (probably from a range of models!). For SAMPEX, L was calculated based on a simple dipole model. For the geostationary satellites LT was used instead of MLT, and a fixed L of 6.6 was used.
4. Transformation of fluxes to equatorial where all done on the assumption of omni-directional flux, flat pitch angle distribution, scaling by B/B_0. This is especially problematic for SAMPEX.

We realize that the method employed involves many approximations. This study was used as a testbed to set up the methods of putting multi-spacecraft data together and displaying that data. As this already is a complex task we started with the simplest method possible.

We would also like to avoid spending a large amount of time on improving some aspects of the method which might not yield any improvement in performance but are computationally heavy, as we will move to an operational system eventually. The idea here is to start simple, and add complexity only where useful.

3. The geostationary synthesis

As a first step we constructed the geostationary synthesis which is used as a baseline for the full synthesis. Data is most dense at geostationary orbit, allowing a very high time resolution for each "ring" of data. Here we take 5 min averages at each satellite and step in 1 min increments.

Fig. 2 shows this for the first compression in the 10 January, 1997 event. Over-plotted with color coded lines are the tracks in local time vs time of the satellites providing the input data for this plot. It can be clearly seen that this event was strongest near 15 hs local time, which also happened to be the location of the TELSTAR satellite that failed at this time.

Satellites near 3 h local time didn't see an event at all, and were thus not affected by this storm. This already shown the importance of global MLT coverage — the dose a given satellite receives very much depends on it's location and its phase with respect to an event.

Reeves et al. (1998) have shown that this flux increase is consistent with an adiabatic compression of the front-side magnetosphere following a large density pulse in the solar wind. The more normal increase of relativistic electrons after $\sim$5 days is not shown here.

Fig. 2 still show some bias of the data along the satellite tracks, showing that even 5 satellites do not provide detailed enough coverage. The observed asymmetry of the fluxes with MLT are at least in part due to the distortion of the magnetic field during disturbed times, when the satellites are no longer close to the same drift shell. Further work is needed here.

4. Full synthesis example

We present here an active period showing three steps involved in constructing a synthesis map.

In Fig. 3 we show the orbital paths projected to the equatorial plane with the color coded flux intensities plotted along each trace. In these plots the geostationary "ring" is constructed first, and then only those data from satellites that have geostationary crossings in the time period chosen are added, their data scaled to agree with their geostationary intersect.

From the "raw data" plot in Fig. 3 we can see one region near $L = 5$ and MLT $= 7$ which is covered be four satellites. All satellites yield very similar flux levels, showing some confidence in the methods used here.

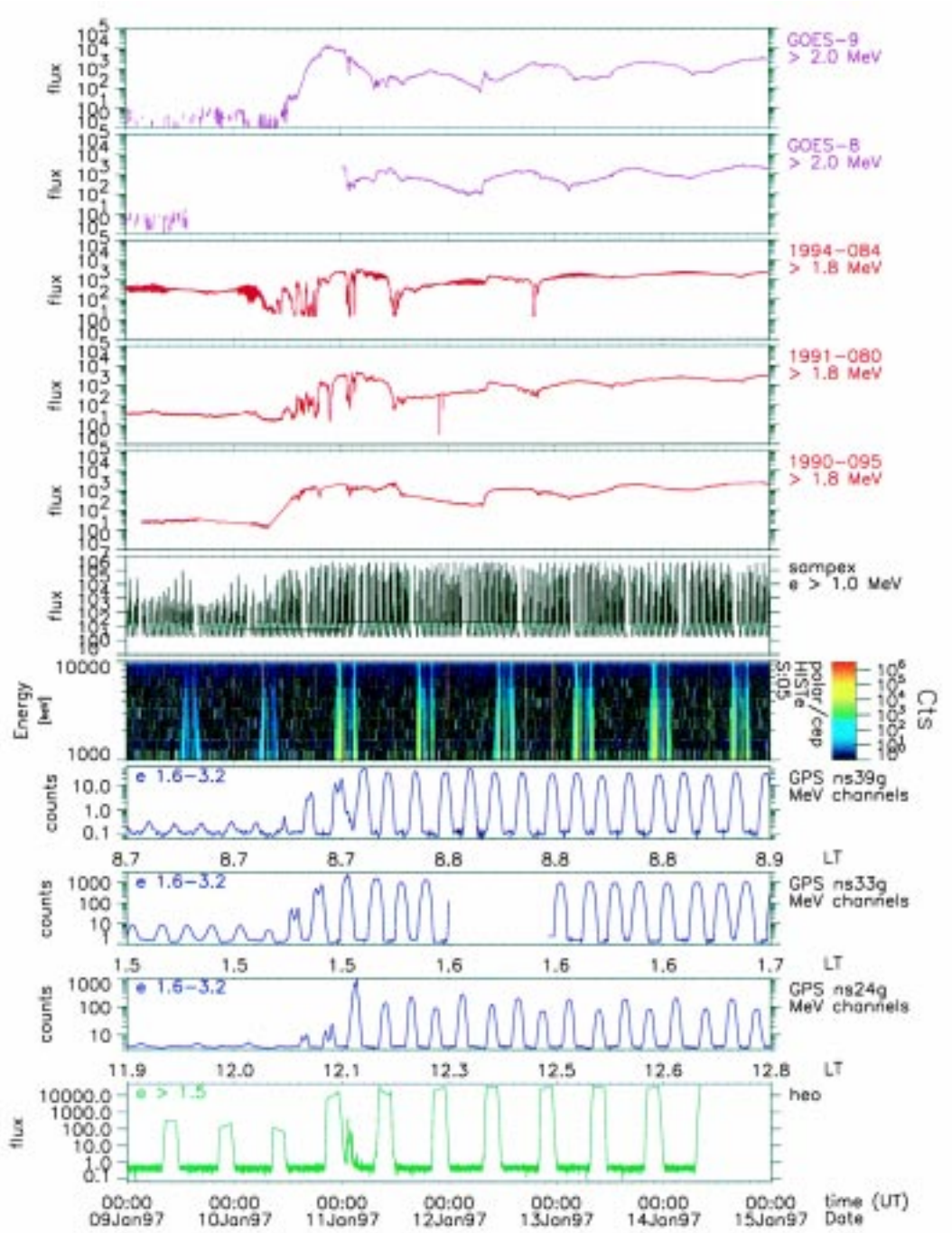

Fig. 1. Time series synthesis input data.

In Fig. 4 the data are binned into an L/MLT (0.5 by 1) grid, averaging together all contributions in a given cell. One can see that even with this number of satellites the actual data coverage is still sparse.

In Fig. 5 data is interpolated along L-shells. Where there is only one filled cell for a given L-shell, that flux is used for the whole L-shell. This completes the construction of the synthesis map.

The flux increase at the initial compression of the magnetosphere (Reeves et al., 1997a) is shown to be locally confined in both L and MLT, peaking just below geostationary orbit and confined to dawn —

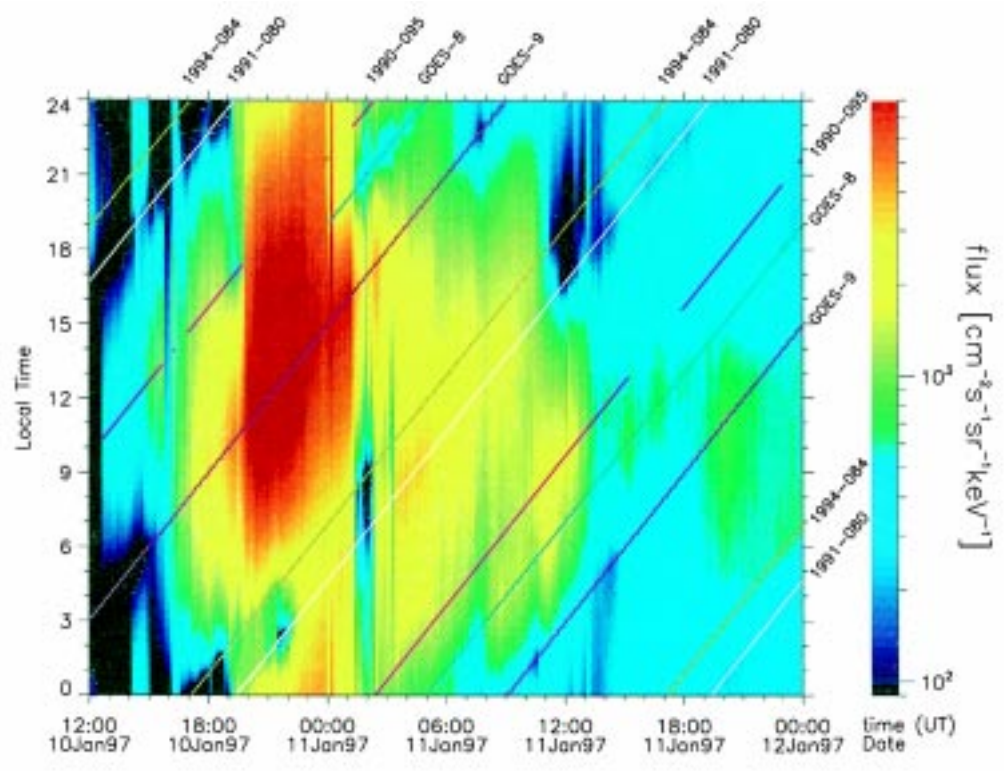

Fig. 2. Fluxes at geostationary orbit at all local times based on 5 geostationary measurements.

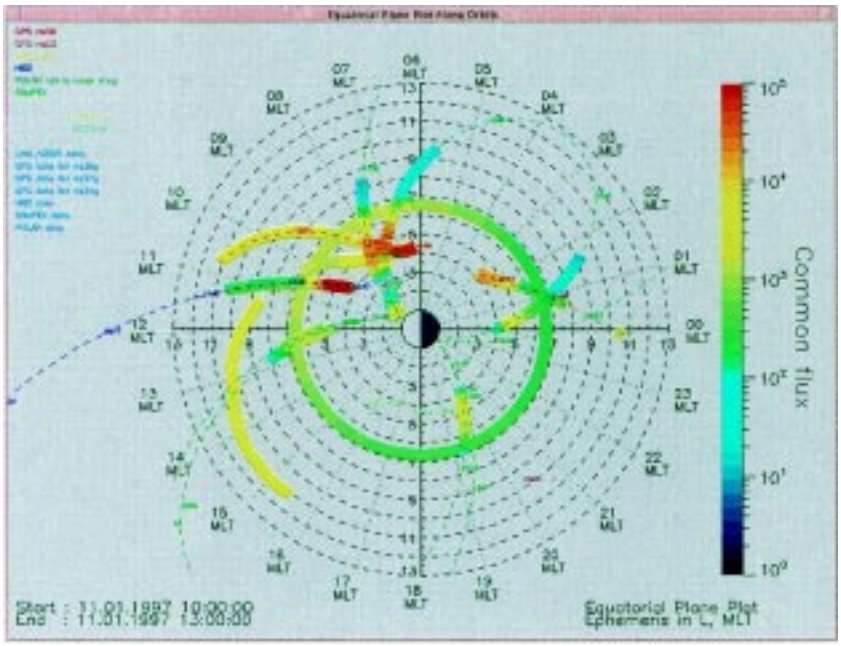

Fig. 3. Active period, orbit plot number of satellites the actual data coverage is still sparse.

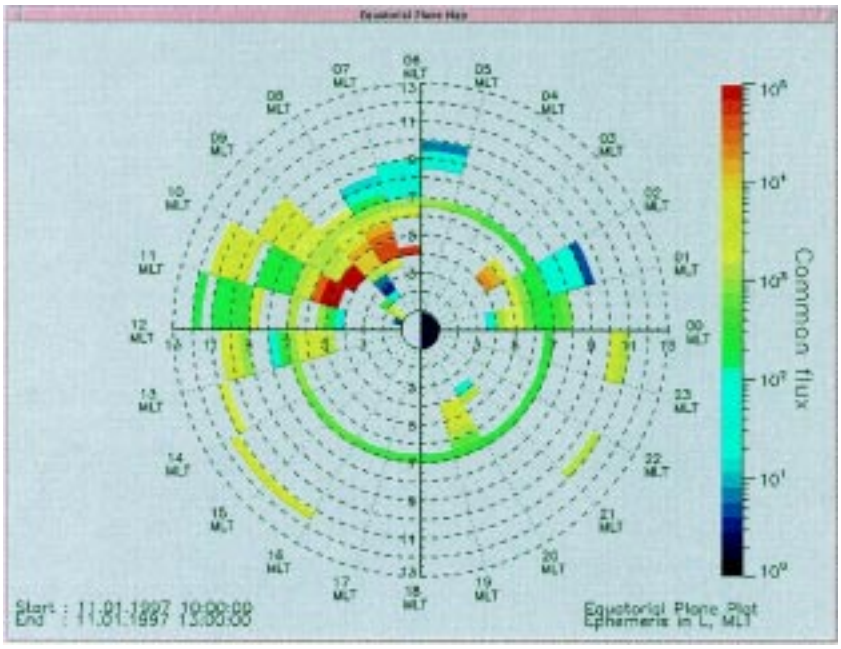

Fig. 4. Active period, binned data.

noon local times. The rest of the magnetosphere is virtually unaffected apart from a flux *decrease* seen from 6–01 MLT and at 7–9 *L*. This indicated a highly localized distortion of the magnetosphere in response to this particular solar wind driver.

5. Caveats on results

As in any temporal and spatial sampling scheme, the ultimate results are as good as the sampling density in both space and time. The data used here was from an

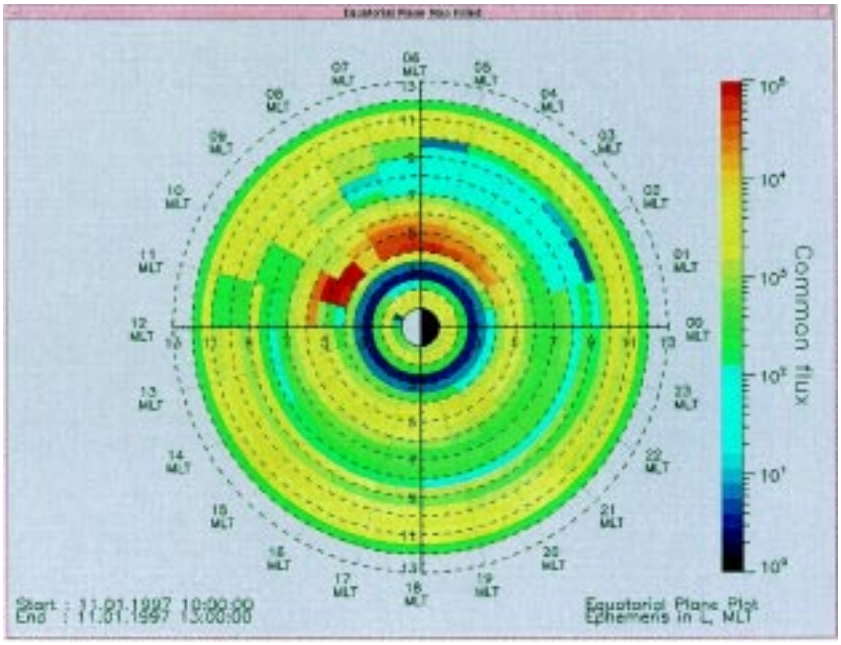

Fig. 5. Active period, full synthesis.

active period not out of design, but because this was a much studied period and data was available! The example shown here serves well to show the limitations of the method during active times.

The basic sampling interval here is 3 h, and there are clearly times during this period when the environment changed at a rate faster than this. Also, the spatial sampling is governed by what satellites happen to be "around", and is highly variable from interval to interval, with times of clustering such as seen in 3 to other times when data coverage is more uniform.

We used this interval to test out the general method used, but make no claim to have found a 100% accurate picture of the 2 MeV environment at ALL the times during this period.

For the examples shown here in Figs. 3–5 these problems are clearly apparent. The absence of spatial structure in the 16–22 local time sectors does not necessarily mean the fluxes where smooth here, but only that the observations are not dense enough in the region as can be seen from Fig. 3 From a time sampling point of view, this method assumes that any flux variations in the sampling window are spatial. The condition of time stationarity is clearly violated during active times, where time-aliasing effects such as substorms can lead to fake spatial gradients.

Given these considerations a given final flux map, even though based on as much data as possible, can still be quite misleading in some areas and for some times. We intent to produce two accompanying maps for each full synthesis map, one showing the density of data points and the other a variability index for the sampling period, so that the user can have some idea if the fidelity of the map.

6. Results — conclusion

We have shown here a first attempt at putting together data from a large number of satellites to provide a global snapshot of the state of the relativistic electron magnetosphere. Even given the many approximations used here the approach taken is clearly useful and already provides new insights into the dynamics during storms with the large local time asymmetries observed. For the first compressional pulse of the 10 January, 1997 magnetic cloud event the relativistic electron enhancement is very localized in both MLT and L.

Limitations on the data and ordering parameters are acceptable at this stage of development of the synthesis model. Refinements are of course infinitely possible, but should only be attempted if the effort required is justified by a real gain in synthesis fidelity.

6.1. Future work

We intend to use the UNIRAD package BLXTRA (Heynderickx et al., 1996) to calculate common L, MLT and Magnetic Latitude for all spacecraft ephemeris using a common magnetic field model. This is in process for a static T89. Dynamic models using real-time input from solar wind monitors such as WIND or ACE would be the next step.

The geostationary reference "ring" needs to be adjusted to truly represent a common L and not R_e. This can be done by using model radial flux gradients to scale all data to the same L.

For many of the instruments further work is needed to obtain a calibrated common flux >2 MeV channel. Here we are dependent on the instrument principal investigators.

A better mapping algorithm is needed between observed fluxes and the reference equatorial plane. This can be achieved in several ways:

1. Using a theoretical model such as the particle transport code SALAMMBO (Beutier and Boscher, 1995; Bourdarie et al., 1997)
2. Using a statistical model such as AE-8, or CRRES-based models through UNIRAD.
3. Establishing a data base of mapping factors from flux (MagLat), L to flux (equatorial).

Near real time Web access to simplified synthesis plots based only on LANL, GOES and GPS is planned.

6.2. More satellites

To improve coverage and lower the time needed to assemble a given synthesis map the only solution is to use more data from more satellites:

1. Sampex is currently the only satellite covering the inner zone below $L = 4$. It has a high time resolution for L-traverses and is crucial for the global synthesis, but is the most critical in transforming to equatorial flux. More inner magnetosphere missions are needed!
2. The full compliment of 12 GPS satellites will eventually have space environment monitors.
3. Using all three HEO spacecraft routinely. Data access here is limited through The Aerospace Corporation. The HEO spacecraft are all on a common MLT orbit, which helps in reducing the time required for a given pass through L.
4. EQUATOR-S for its short life period (Data from January 1997 to April 1998) was in an elliptical, near-equatorial orbit (11 R_e by 500 km), yielding one radiation belt traverse every 21 h.

References

Baker, D.N., Mason, G.M., Figueroa, O., Colon, G., Watzin, J., Aleman, R.M., 1993. An overview of the solar, anomalous, and magnetospheric particle explorer (SAMPEX) mission. IEEE Transactions onGeoscience and Remote Sensing 31, 531–541.

Beutier, T., Boscher, D., 1995. A three-dimensional analysis of the electron radiation belt by the salammbo code. J. Geophys. Res. 100, 14,853–14,861.

Blake, B.J., Fennell, J.F., Friesen, L.M., Johnson, B.M., Kolasinski, W.A., Mabry, D.J., Osborn, J.V., Penzin, S.H., Schnauss, E.R., Spence, H.E., Baker, D.N., Belian, R., Fritz, T.A., Ford, W., Laubscher, B., Stiglich, R., Baraze, R.A., Hilsenrath, M.F., Imhof, W.L., Kilner, J.R., Mobilia, J., Voss, H.D., Korth, A., Güll, M., Fischer, K., Grande, M., Hall, D., 1995. CEPPAD: comprehensive energetic particle and pitch angle distribution experiment on POLAR. Space Sci. Rev. 71, 531.

Blake, J.B., Baker, D.N., Turner, N., Ogilvie, K.W., Lepping, R.P., 1997. Correlation of changes in the outer-zone relativistic-electron population with upstream solar wind and magnetic field measurements. Geophys. Res. Letters 24, 927.

Bourdarie, S., Boscher, D., Beutier, T., Sauvaud, J-A., Blane, M., 1997. Electron and proton radiation belt dynamic simulations during storm periods: a new asymmetric convection-diffusion model. J. Geophys. Res. 102, 17,541–17,552.

Feldman, W., Aiello, W., Drake, D., Herrin, M., 1985. The BDD II: an improved electron dosimeter for the global positioning system. Technical Report LA-10453-MS, Los Alamos National Laboratory, Los Alamos, NM 87545, USA.

Friedel, R.H.W., Korth, A., 1994. Observations of energetic particle population in the inner magnetosphere over the whole CRRES mission. In: Baker, H.O., Baker, D. (Eds.), Proceedings of the Eighth International Symposium on Solar Terrestrial Physics. Terra Scientific, Tokyo.

Friedel, R.H.W., Korth, A., 1995. Long-term observations of kev ion and electron variability in the outer radiation belt from CRRES. Geophys. Res. Letters 22, 1853–1856.

Friedel, R.H.W., Korth, A., 1996. A dynamic data driven radiation belt model based on CRRES data. In: Proceedings of the Symposium on Environment Modelling for Space-Based Applications, SP-392. ESA. ESA Publications Division, ESTEC, Noordwijk, The Netherlands.

Heynderickx, D., Kruglanski, M., Lemaire, J., 1996. UNIRAD v 3.0 Trapped radiation Software User Manual. Ringlaan 3, B-1180 Brussel, Belgium.

Korth, A., Friedel, R.H.W., Mouikis, C., Fennell, J.F., 1998. Storm/Substorm signatures in the outer radiation belt. In: Proceedings of the 4th International Conference on Substorms. Terra Scientific, Tokyo.

Reeves, G.D., Baker, D.N., Belian, R.D., Blake, J.B., Cayton, T.E., Fennell, J.F., Friedel, R.H.W., Li, X., Meier, M.M., Selesnik, R.S., Spence, H.E., 1998. The global response of relativistic radiation belt electrons to the January 1997 magnetic cloud. Geophys. Res. Letters, 25, 3265–3268.

Reeves, G.D., Belian, R.D., Cayton, T.C., Henderson, M.G., Christensen, R.A., McLachlan, P.S., Ingraham, J.C., 1997. Using Los Alamos geosynchronous energetic particle data in support of other missions. In: Lockwood, M., Opgenoorth, H.J., Wild, M.N., Stampe, R. (Eds.), Satellite-Ground Based Coordination Source book, pp. 263–272.

Space-Systems-Loral, 1996. GOES I-M Databook, Revision 1, Chapter Space Environment Monitor Subsystem. Systems-Loral, pp. 58–66.

Vette, J.L., 1991. The NASA/National Space Science Data Center trapped radiation environment model program (1964–1991). Technical Report NSSDC/WDC-A-R & 91-26, Goddard Space FlightCenter, NASA/GSFC, Greenbelt, USA.